INTERACTING MULTIPLE MODEL ADAPTIVE UNSCENTED KALMAN FILTERS FOR NAVIGATION SENSOR FUSION

National Taiwan Ocean University
Dah-Jing Jwo*, Mu-Yen Chen*, Chien-Hao Tseng **
* National Taiwan Ocean University, Taiwan
** National Center for High-Performance Computing, Taiwan

Abstract

The unscented Kalman filter (UKF) is adopted in the interacting multiple model (IMM) framework to deal with the system nonlinearity in navigation applications. The adaptive tuning system (ATS) is employed for assisting the unscented Kalman filter in the IMM framework, resulting in an interacting multiple model adaptive unscented Kalman filter (IMM-AUKF). Two models, a standard UKF and an adaptive UKF (AUKF), are used in the IMM for dynamically adjusting the process noise to enhance the estimation accuracy and tracking capability. Accuracy comparison on navigation sensor fusion for AUKF, IMM-UKF, and IMM-AUKF approaches are presented. Furthermore, a performance measure referred to as the Instability Index (ISI) is introduced to evaluate the stability influenced by time-varying dynamics characteristics. Among the three approaches, the IMM-AUKF approach has the best overall positioning performance. Unlike the IMM-UKF, both IMM-AUKF and AUKF have equivalently good ISI values, indicating that positioning accuracies by the two methods are relatively reliable under the change of dynamics characteristics.

1 Introduction

The extended Kalman filter (EKF) [1,2] has been shown to be a minimum mean square error estimator. Unfortunately, the fact that EKF highly depends on a predefined dynamics model forms a major drawback. For achieving good filtering results, the designers are required to have the complete *a priori* knowledge on both the dynamic process and measurement models, in addition to the assumption that both the process and measurement are corrupted by zero-mean Gaussian white sequences. The adaptive Kalman filter algorithm [3,4] has been one of the strategies considered for estimating the state vector to prevent divergence problem due to modeling errors. Moreover, the calculation of the Jacobian matrices makes it difficult to implement, especially for non-differentiable function.

The interacting multiple model (IMM) algorithm [5,6] has the configuration that runs in parallel several model-matched state estimation filters, which exchange information (interact) at each sampling time. The of IMM algorithm has been originally applied to target tracking [7-9], and recently extended to GPS navigation [10,11]. A model probability evaluator calculates the current probability of the vehicle being in each of the possible modes. A global estimate of the vehicle's state is computed using the latest mode probabilities. This algorithm carries out a soft-switching between the various modes by adjusting the probabilities of each mode, which are used as weightings in the combined global state estimate. The covariance matrix associated with this combined estimate takes into account the covariances of the mode-conditioned estimates as well as the differences between these estimates. The AKF approach is based on parametric adaptation, while the IMM approach is based on filter structural adaptation (model switching).

The unscented Kalman filter (UKF) is a nonlinear, distribution approximation method, which uses a finite number of sigma points to

propagate the probability of state distribution through the nonlinear dynamics of system. The UKF made a Gaussian approximation with a limited number of points (sigma points) by using the Unscented Transform (UT) [12-15]. The deterministic sampling approach is used to capture the mean and covariance estimates with a minimal set of samples, and the posterior mean and covariance undergoing a nonlinear propagation can be calculated accurately at least to the second order.

The UKF naturally suffers the same problem as the EKF. The uncertainty of the process noise and measurement noise will degrade the performance of UKF. An adaptive mechanism which dynamically identifies uncertainties or modeling errors can be adopted. To deal with noise uncertainty and system nonlinearity simultaneously, the IMM-UKF can be introduced. In the approach, multiple models are developed to describe various dynamic behaviors. In each model an UKF is running, and the IMM algorithm makes uses of model probabilities to weight the inputs and output of a bank of parallel filters at each time instant. By monitoring the innovation information, the IMM-UKF augmented by an adaptive tuning system (ATS), referred to the IMM-AUKF herein, is employed for dynamically adjusting the process noise for further enhancing the estimation accuracy and tracking capability.

The Global Positioning System (GPS) [1,16] and inertial navigation system (INS) have complementary operational characteristics and the synergy of both systems has been widely explored. The GPS/INS integrated navigation system, typically carried out through the EKF, is the adequate solution to provide a navigation system that has superior performance in comparison with either GPS or INS stand-alone system. The example on loosely-coupled GPS/INS integrated navigation processing based on the IMM-AUKF will be presented. Performance improvement will be demonstrated using the proposed IMM-AUKF method as compared to the AUKF and IMM-UKF approaches.

This paper is organized as follows. In Section 2, preliminary background on the IMM-UKF is discussed. The proposed sensor fusion strategy is introduced in Section 3. In Section 4, navigation integration application is carried out to evaluate the performance of the proposed approach. Conclusions are given in Section 5.

2 The Interacting Multiple Model Unscented Kalman Filter

The unscented Kalman filtering deals with the case governed by the nonlinear stochastic difference equations:

$$\mathbf{x}_{k+1} = f(\mathbf{x}_k, k) + \mathbf{w}_k \qquad (1a)$$

$$\mathbf{z}_k = h(\mathbf{x}_k, k) + \mathbf{v}_k \qquad (1b)$$

where the state vector $\mathbf{x}_k \in \mathfrak{R}^n$, process noise vector $\mathbf{w}_k \in \mathfrak{R}^n$, measurement vector $\mathbf{z}_k \in \mathfrak{R}^m$, and measurement noise vector $\mathbf{v}_k \in \mathfrak{R}^m$. The vectors $\mathbf{w}_k$ and $\mathbf{v}_k$ are zero mean Gaussian white sequences having zero cross-correlation with each other:

$$\mathbf{E}[\mathbf{w}_k \mathbf{w}_i^{\mathrm{T}}] = \begin{cases} \mathbf{Q}_k, & i = k \\ 0, & i \neq k \end{cases}; \ \mathbf{E}[\mathbf{v}_k \mathbf{v}_i^{\mathrm{T}}] = \begin{cases} \mathbf{R}_k, & i = k \\ 0, & i \neq k \end{cases};$$

$$\mathbf{E}[\mathbf{w}_k \mathbf{v}_k^{\mathrm{T}}] = \mathbf{0} \ \textit{for all i and k}$$

where $\mathbf{Q}_k$ is the process noise covariance matrix, $\mathbf{R}_k$ is the measurement noise covariance matrix.

Instead of linearizing using Jacobian matrices as in the EKF and achieving first-order accuracy, the UKF uses a deterministic sampling approach to capture the mean and covariance estimates with a minimal set of sample points. The UKF was first proposed by Julier, et al. [17] to address nonlinear state estimation in the context of control theory. When the sample points are propagated through the true nonlinear system, the posterior mean and covariance can be captured accurately to the 3rd order of Taylor series expansion for any nonlinear system. One of the remarkable merits is that the overall computational complexity of the UKF is the same as that of the EKF [18].

The first step in the UKF is to sample the prior state distribution, i.e., generate the sigma points through the UT, which is a method for calculating the statistics of a random variable which undergoes a nonlinear transformation. The basic premise is that to approximate a probability distribution is easier than to approximate an arbitrary nonlinear

transformation. The samples are propagated through true nonlinear equations, and the linearization of the model is not required.

Suppose the mean $\bar{\mathbf{x}}$ and covariance $\mathbf{P}$ of vector $\mathbf{x}$ are known, a set of deterministic vector called sigma points can then be found. The ensemble mean and covariance of the sigma points are equal to $\bar{\mathbf{x}}$ and $\mathbf{P}$. The nonlinear function $\mathbf{y} = f(\mathbf{x})$ is applied to each deterministic vector to obtain transformed vectors. The ensemble mean and covariance of the transformed vectors will give a good estimate of the true mean and covariance of $\mathbf{y}$, which is the key to the unscented transformation. The UKF approach estimates are expected to be closer to the true values than the EKF approach.

The sigma vectors are propagated through the nonlinear function to yield a set of transformed sigma points,

$$\mathbf{y}_i = f(\mathbf{X}_i) \quad i = 0,...,2n \quad (2)$$

The mean and covariance of $\mathbf{y}_i$ are approximated by a weighted average mean and covariance of the transformed sigma points as follows:

$$\bar{\mathbf{y}}_u = \sum_{i=0}^{2n} W_i^{(m)} \mathbf{y}_i \quad (3)$$

$$\bar{\mathbf{P}}_u = \sum_{i=0}^{2n} W_i^{(c)} (\mathbf{y}_i - \bar{\mathbf{y}}_u)(\mathbf{y}_i - \bar{\mathbf{y}}_u)^T \quad (4)$$

As compared to the EKF's linear approximation, the unscented transformation is accurate to the second order for any nonlinear function.

The IMM-UKF algorithm uses model (Markov chain state) probabilities to weight the input and output of a bank of parallel UKFs at each time instant. The approach takes into account a set of models to represent the system behavior patterns or system model. The overall estimates is obtained by a combination of the estimates from the filters running in parallel based on the individual models that match the system modes. Each cycle consists of four major steps: interaction (mixing), filtering, mode probability calculation, and estimate combination. One cycle of IMM-UKF can be written as follows:

1. Model interaction/mixing

For given target states $\mathbf{x}_{k-1}^j = \mathbf{x}_{k-1|k-1}^j$ with corresponding covariances $\mathbf{P}_{k-1}^j = \mathbf{P}_{k-1|k-1}^j$ and mixing probabilities $\mu_{k-1|k-1}^{i|j}$ for every model, an initial estimate-covariance pair is given by:

$$\hat{\mathbf{x}}_{k-1|k-1}^{0j} = \sum_{i=1}^{r} \hat{\mathbf{x}}_{k-1|k-1}^i \mu_{k-1|k-1}^{i|j}, \quad j = 1,2,...,r \quad (5)$$

$$\mathbf{P}_{k-1|k-1}^{0j} = \sum_{i=1}^{r} \mu_{k-1|k-1}^{i|j} \{ \mathbf{P}_{k-1|k-1}^i + [\hat{\mathbf{x}}_{k-1|k-1}^i - \hat{\mathbf{x}}_{k-1|k-1}^{0j}][\bullet]^T \} \quad (6)$$

The model transition probabilities, which are related to Markov chain, are defined as:

$$\pi_{ij} = p\{M_k^j \mid M_{k-1}^i\}$$

$$= \begin{bmatrix} \pi_{11} & \pi_{12} & \cdots & \pi_{1j} \\ \pi_{21} & \pi_{22} & \cdots & \pi_{2j} \\ \vdots & \vdots & \ddots & \vdots \\ \pi_{i1} & \pi_{i2} & \cdots & \pi_{ij} \end{bmatrix}$$

where $i, j = 1,2,...,r$, and r is the number of sub-models. Calculating the mixing probabilities with mode switching probability matrix π_{ij} and the Gaussian mixing probabilities are computed via the equations

$$\mu_{k-1|k-1}^{i|j} = \frac{1}{\bar{\mathbf{c}}_j} \pi_{ij} \mu_{k-1}^i \quad (7)$$

where $\bar{\mathbf{c}}_j$ is a normalization factor is

$$\bar{\mathbf{c}}_j = \sum_{i=1}^{r} \pi_{ij} \mu_{k-1}^i \quad (8)$$

2. Model individual filtering
- *Step 1 in UKF loop.* The unscented transform creates $2n+1$ sigma vectors $\mathbf{X}$ (a capital letter) and weighted points W. For state estimation at instant $k-1$, sigma points are generated according to

$$\begin{cases} \mathbf{X}_{0,k-1}^j = \hat{\mathbf{x}}_{k-1}^{0j} \\ \mathbf{X}_{i,k-1}^j = \hat{\mathbf{x}}_{k-1}^{0j} + (\sqrt{(n+\lambda)\mathbf{P}_{k-1}^{0j}})_i^T \\ \mathbf{X}_{i+n,k-1}^j = \hat{\mathbf{x}}_{k-1}^{0j} - (\sqrt{(n+\lambda)\mathbf{P}_{k-1}^{0j}})_i^T \end{cases} , \quad i = 1,...,n \quad (9)$$

where $(\sqrt{(n+\lambda)\mathbf{P}_{k-1}^{0j}})_i$ is the ith row (or column) of the matrix square root. $\sqrt{(n+\lambda)\mathbf{P}_{k-1}^{0j}}$ can be obtained from the lower-triangular matrix of the Cholesky factorization; $\lambda = \alpha^2(n+k) - n$ is a scaling parameter used to control the covariance matrix; α determines the spread of the sigma points and is usually set to a small positive $(e.g., 1e-4 \leq \alpha \leq 1)$; k is a secondly scaling parameter (usually set as 0); β is used to incorporate prior knowledge of the distribution

of $\bar{\mathbf{x}}$ (When $\mathbf{x}$ is normally distributed, $\beta = 2$ is an optimal value); $W_i^{(m)}$ is the weight for the mean associated with the ith point; and $W_i^{(c)}$ is the weigh for the covariance associated with the ith point.

$$W_0^{(m)} = \frac{\lambda}{(n+\lambda)} \qquad (10a)$$

$$W_0^{(c)} = W_0^{(m)} + (1 - \alpha^2 + \beta) \qquad (10b)$$

$$W_i^{(m)} = W_i^{(c)} = \frac{1}{2(n+\lambda)}, \quad i = 1,...,2n \qquad (10c)$$

- *Step 2 in UKF loop.* Time update (prediction steps)

$$\zeta_{i,k|k-1}^j = f_j(\mathbf{X}_{i,k-1}^j), \ i = 0,...,2n \qquad (11)$$

$$\hat{\mathbf{x}}_{k|k-1}^j = \sum_{i=0}^{2n} W_i^{(m)} \zeta_{i,k|k-1}^j \qquad (12)$$

$$\mathbf{P}_{k|k-1}^j = \sum_{i=0}^{2n} W_i^{(c)} [\zeta_{i,k|k-1}^j - \hat{\mathbf{x}}_{k|k-1}^j][\zeta_{i,k|k-1}^j - \hat{\mathbf{x}}_{k|k-1}^j]^T + \mathbf{Q}_{k-1}^j \qquad (13)$$

$$\mathbf{Z}_{i,k|k-1}^j = h(\zeta_{i,k|k-1}^j) \qquad (14)$$

$$\hat{\mathbf{z}}_{k|k-1}^j = \sum_{i=0}^{2n} W_i^{(m)} \mathbf{Z}_{i,k|k-1}^j \qquad (15)$$

- *Step 3 in UKF loop.* Measurement update (correction steps)

$$\mathbf{P}_{zz}^j = \sum_{i=0}^{2n} W_i^{(c)} [\mathbf{Z}_{i,k|k-1}^j - \hat{\mathbf{z}}_{k|k-1}^j][\mathbf{Z}_{i,k|k-1}^j - \hat{\mathbf{z}}_{k|k-1}^j]^T + \mathbf{R}_k^j \qquad (16)$$

$$\mathbf{P}_{xz}^j = \sum_{i=0}^{2n} W_i^{(c)} [\zeta_{i,k|k-1}^j - \hat{\mathbf{x}}_{k|k-1}^j][\mathbf{Z}_{i,k|k-1}^j - \hat{\mathbf{z}}_{k|k-1}^j]^T \qquad (17)$$

$$\mathbf{K}_k^j = \mathbf{P}_{xz}^j (\mathbf{P}_{zz}^j)^{-1} \qquad (18)$$

$$\hat{\mathbf{x}}_{k|k}^j = \hat{\mathbf{x}}_{k|k-1}^j + \mathbf{K}_k^j \mathbf{v}_k^j, \text{ where } \mathbf{v}_k^j = \mathbf{z}_k - \hat{\mathbf{z}}_{k|k-1}^j \qquad (19)$$

$$\mathbf{P}_{k|k}^j = \mathbf{P}_{k|k-1}^j - \mathbf{K}_k^j \mathbf{P}_{zz}^j \mathbf{K}_k^{jT} \qquad (20)$$

The samples are propagated through true nonlinear equations; the linearization is unnecessary (Calculation of Jacobian is not required). They can capture the states up to at least second order, where as the EKF is only a first order approximation.

3. Model probabilities update

Model probability $\boldsymbol{\mu}_k^j$ is updated according to the model likelihood and model transition probability governed by the finite-state Markov chain:

$$\boldsymbol{\mu}_k^j = \frac{1}{c} \Lambda_k^j \bar{\mathbf{c}}_j \qquad (21)$$

where the normalized constant and

$$c = \sum_{j=1}^r \bar{\mathbf{c}}_j \Lambda_k^j \qquad (22)$$

$$\Lambda_k^j = \frac{1}{\sqrt{2\pi |\mathbf{P}_{zz}^j|}} \exp\left[-\frac{1}{2} \mathbf{v}_k^{jT} (\mathbf{P}_{zz}^j)^{-1} \mathbf{v}_k^j\right] \qquad (23)$$

4. Combination of state estimation and covariance combination

The model-individual estimates and covariances are combined to an overall state and covariance.

$$\hat{\mathbf{x}}_{k|k} = \sum_{j=1}^r \hat{\mathbf{x}}_{k|k}^j \boldsymbol{\mu}_k^j \qquad (24)$$

$$\mathbf{P}_{k|k} = \sum_{j=1}^r \boldsymbol{\mu}_k^j \{\mathbf{P}_{k|k}^j + [\hat{\mathbf{x}}_{k|k}^j - \hat{\mathbf{x}}_{k|k}][\bullet]^T\} \qquad (25)$$

3 The Proposed Sensor Fusion Strategy

Fig. 1 shows the block diagram of the proposed IMM-AUKF algorithm. Two models are used in the IMM configuration: a standard (non-adaptive) UKF and an adaptive UKF (AUKF). To account for the modeling error or statistic uncertainties, the UKF is augmented by an ATS for determining the process noise covariance $\mathbf{Q}_k$ of the AUKF, which is then the upper bound of process noise covariance in the IMM. The ATS is designed according to the innovation information, and then adjust the bandwidth of the IMM filter through reducing or increasing the upper bound of the process noise covariance. For timely reflecting the change in vehicle dynamics, the degree of divergence (DOD) parameter ξ is defined as the normalized innovation squared value at the present epoch:

$$\xi = \mathbf{v}_k^T \mathbf{P}_{zz}^{-1} \mathbf{v}_k \qquad (26)$$

where $\mathbf{v}_k = [v_1 \ v_2 \ ... \ v_m]^T$, m is the number of measurements. This statement is equivalent to the trace of the practical innovation covariance divided by the theoretical one. Furthermore, the DOD parameter ξ follows the Chi-square distribution, and the probability of ξ less than its expectation value will be always larger than 50%.

The innovation reflects the discrepancy between the predicted measurement and the actual measurement. It represents the additional information available to the filter as a

consequence of the new observation. As the statistical sample variance estimate of $\mathbf{P}_{zz}$, matrix the $\hat{\mathbf{P}}_{zz}$ can be computed through averaging inside a moving estimation window

$$\hat{\mathbf{P}}_{zz} = \frac{1}{M} \sum_{j=j_0}^{k} \mathbf{v}_j \mathbf{v}_j^{\mathrm{T}} \qquad (27)$$

where M is the number of samples (usually referred to the window size); $j_0 = k - M + 1$ is the first sample inside the estimation window. The benefit of the adaptive algorithm is that it keeps the covariance consistent with the real performance. The innovation sequences have been utilized by the correlation and covariance-matching techniques to estimate the noise covariances. The basic idea behind the covariance-matching approach is to make the actual value of the covariance of the residual consistent with its theoretical value. The estimate of process noise $\mathbf{Q}_k$ is calculated through

$$\hat{\mathbf{Q}}_k \approx \mathbf{K}_k \hat{\mathbf{P}}_{zz} \mathbf{K}_k^{\mathrm{T}} \qquad (28)$$

For more detailed information on derivation of these equations, see Mohamed & Schwarz [3].
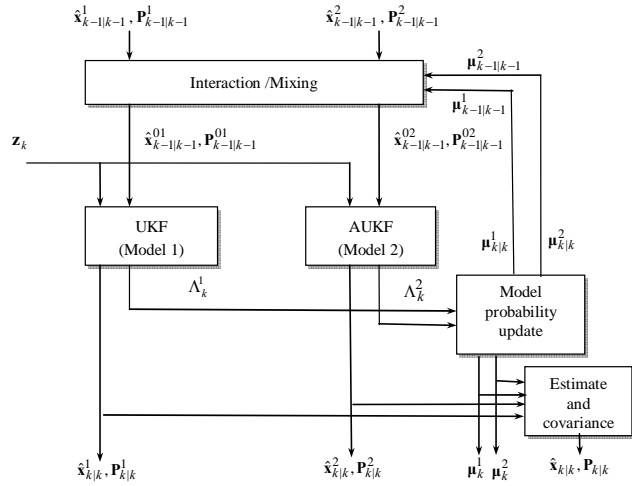
Fig. 1. The block diagram of the IMM-AUKF algorithm (one cycle with two modes).

By monitoring the DOD parameter ξ , the ATS is employed for on-line tuning of the process noise covariance and improves estimation performance. The adaptation rule for the AUKF is given by:

$$\mathbf{Q}_k = \begin{cases} \gamma \mathbf{Q}_L & \text{if } \xi \le \mathrm{E}[\xi] \\ \dfrac{tr(\hat{\mathbf{Q}}_k)}{tr(\mathbf{Q}_L)} \times \mathbf{Q}_L & \text{if } \xi > \mathrm{E}[\xi] \end{cases} \qquad (29)$$

where the estimated process noise covariance $\hat{\mathbf{Q}}_k$ is calculated by (28), and the pre-specified multiplier γ is an adequately large number (e.g. 100 is used in this paper) to ensure two models function properly under the Bayesian exclusive assumption in the IMM.

A smaller process noise covariance $\mathbf{Q}_k$ indicates that the vehicle is in low dynamic motion; while a larger process noise covariance indicates that the vehicle is in high dynamics maneuvering. An adequately small process noise covariance is chosen as the lower bound in the standard UKF ($\mathbf{Q}_L$), which is suitable for the non maneuvering case. The block diagram of the AUKF algorithm is shown in Fig. 2.
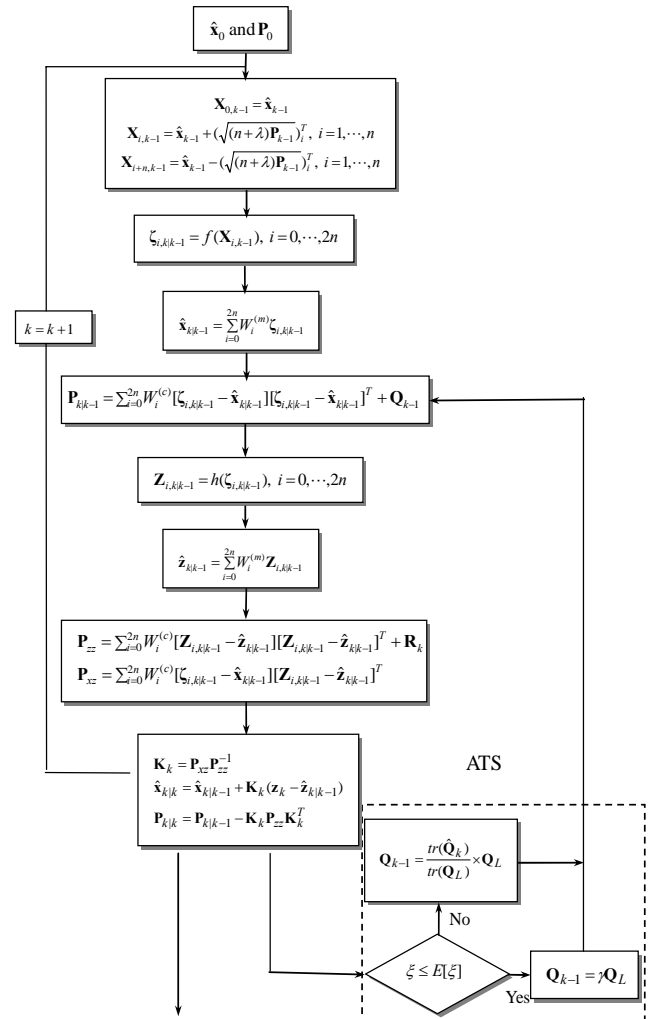
Fig. 2. The block diagram of AUKF.

4 Navigation Integration Performance Evaluation

Simulation experiments were carried out to evaluate the performance of the proposed IMM-AUKF approach in comparison with the IMM-UKF and AUKF methods for GPS/INS navigation sensor fusion. The commercial software Satellite Navigation (SATNAV) Toolbox by GPSoft LLC was employed for generating the satellite positions and pseudoranges. The satellite constellation was simulated and the error sources corrupting GPS measurements include ionospheric delay, tropospheric delay, receiver noise and multipath. It is assumed that the differential GPS mode is used and most of the errors can be corrected, while the multipath and receiver thermal noise cannot be eliminated. Fig. 3 shows the configuration of the loosely-coupled feedback GPS/INS integrated navigation processing using the IMM-AUKF. The measurement is the residual between GPS generated position and INS predicted position.

The differential equations describing the two-dimensional inertial navigation state are:

$$\begin{bmatrix} \dot{n} \\ \dot{e} \\ \dot{v}_n \\ \dot{v}_e \\ \dot{\psi} \end{bmatrix} = \begin{bmatrix} v_n \\ v_e \\ a_n \\ a_e \\ \omega_r \end{bmatrix} = \begin{bmatrix} v_n \\ v_e \\ \cos(\psi)a_u - \sin(\psi)a_v \\ \sin(\psi)a_u + \cos(\psi)a_v \\ \omega_r \end{bmatrix} \quad (30)$$

where $[a_u, a_v]$ are the measured accelerations in the body frame, ω_r is the measured yaw rate in the body frame, as shown in Fig. 4. The error model for INS is augmented by some sensor error states such as accelerometer biases and gyroscope drifts. Actually, there are several random errors associated with each inertial sensor. It is usually difficult to set a certain stochastic model for each inertial sensor that works efficiently at all environments and reflects the long-term behavior of sensor errors. The difficulty of modeling the errors of INS raised the need for a model-less GPS/INS integration technique.
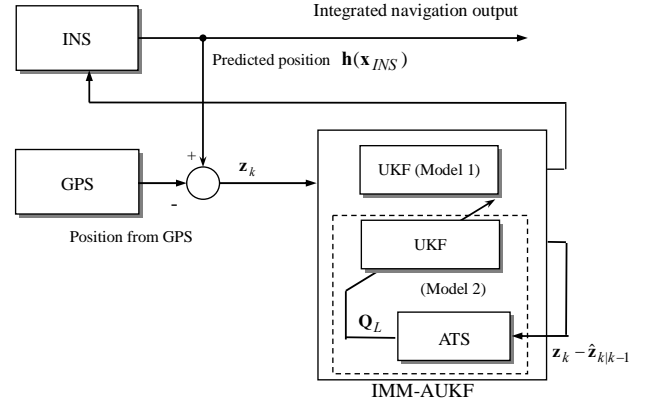
Fig. 3. Configuration of the loosely-coupled feedback integrated navigation using the proposed approach.
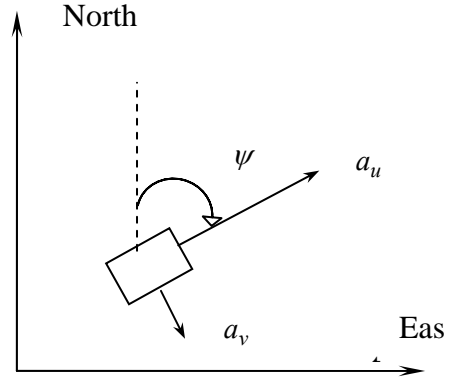
Fig. 4. Illustration of the two-dimensional inertial navigation.

The experiment was conducted on a simulated vehicle trajectory originating from the (0,0,0) m location in the ENU coordinate frame. The simulated sensor outputs for the accelerometers and gyroscope are shown as in Fig. 5. The designed vehicle trajectory covers four categories of dynamic characteristics according to the level of dynamic involved: (1) constant-velocity straight-line during the time intervals, 0-200, 401-600, 901-1200, and 1276-1600s, all at a speed of 10π m/s; (2) counter-clockwise circular motion with radius 1000 meters during 201-400s; (3) clockwise circular motions with radius 2000 meters during 601-900s, and (4) clockwise circular motions with radius 500 meters during 1200-1275s, respectively. The four levels of vehicle dynamics involved are HM (201-400s, medium-high dynamic motion), HL (601-900s, low-high dynamic motion), HH (1200-1275s, high dynamic motion), and L (for the rest of time intervals, low dynamic environments),

respectively. The trajectories for the simulated vehicle (solid) and the unaided INS derived position (dashed) is shown in Fig. 6. Fig. 7 shows the east and north components of INS navigation errors.

The architecture for IMM-AUKF is similar to that of IMM-UKF except that one of the UKFs in IMM-AUKF structure is augmented by the parameter adaptation mechanism (i.e., ATS). The process noise covariance matrices in the IMM-UKF do not change subject to the change in dynamic characteristics, while in the IMM-AUKF, one of the process noise covariance matrices is determined by the ATS. As for the initial value of multiplier (γ), $\gamma = 100$ is chosen (i.e., the pre-specified process noise covariance for Model 2 is set to be 100 times to that of Model 1) for the IMM-AUKF.

The following model transition probability matrices of the Markov chain π_{ij} were assumed:

$$\pi_{ij} = \begin{cases} 0.99 & \text{if } i = j \\ \frac{1-0.99}{N-1} & otherwise \end{cases} \qquad (31)$$

In this paper, $r = 2$, therefore

$$\pi_{ij} = \begin{bmatrix} 0.99 & 0.01 \\ 0.01 & 0.99 \end{bmatrix}$$

The initial model probability for each sub-model is chosen as

$$\mu_0^j = \begin{cases} 0.5 & if\ \text{j} = 1 \\ \frac{1-0.5}{N-1} & otherwise \end{cases} \qquad (32)$$
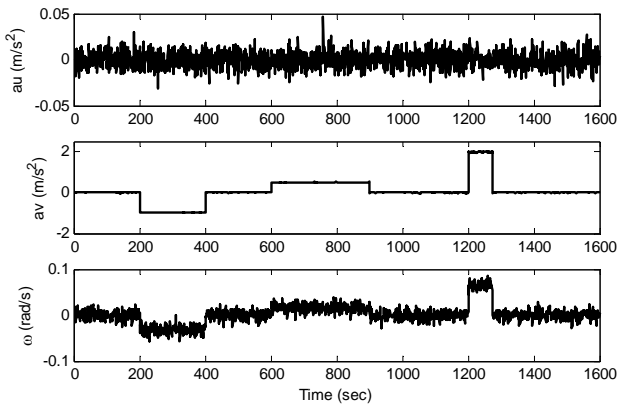
Fig. 5. Simulated sensor outputs for the accelerometers and gyroscope.
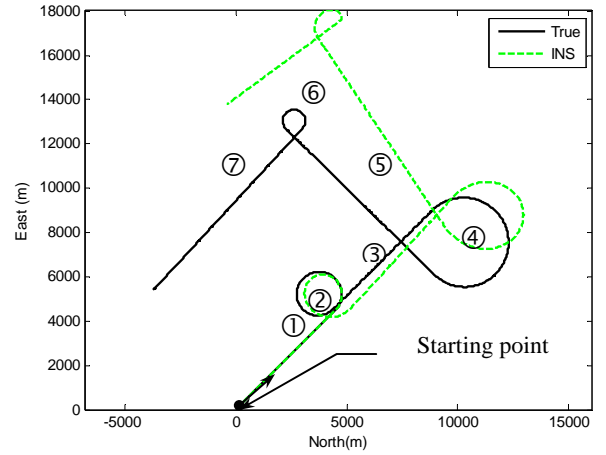
Fig. 6. Trajectory for the simulated vehicle (solid) and the INS derived position (dashed).
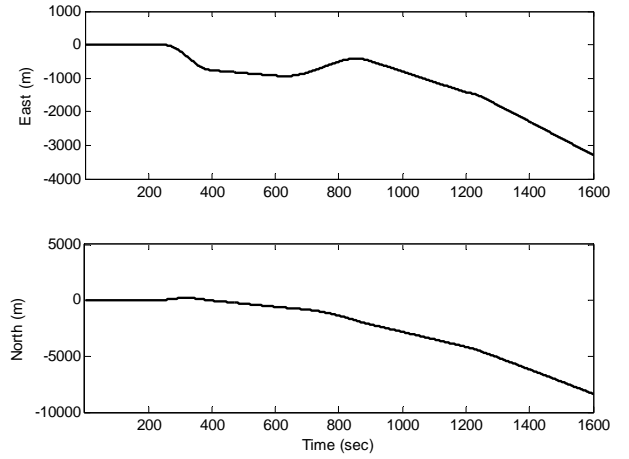
Fig. 7. East and north components of INS navigation errors.

Fig. 8 shows the trajectories of ATS outputs and the corresponding DOD parameter ξ. The resulting model probabilities for the two models obtained by the proposed IMM-AUKF is depicted in Fig. 9. It can be seen that the proposed method adequately capture the change of dynamic characteristics. Results for the IMM-UKF, AUKF, and IMM-AUKF approaches are as follows. The results for the corresponding four levels of dynamics are denoted as E-L, E-HL, E-HM, and E-HH, for the east component; N-L, N-HL, N-HM, and N-HH for the north component, respectively. The overall performance in east and north direction, respectively, is denoted as E and N, respectively, i.e., $E = E\text{-}(L \cup HL \cup HM \cup HH)$, and $N = N\text{-}(L \cup HL \cup HM \cup HH)$. The mean values and standard deviations of positioning errors based on 50 Monte Carlo runs are illustrated in Figs.

10-11, and summarized in Table 1. It can be seen that substantial accuracy improvement is achieved by the proposed method.

In addition, a dimensionless performance measure referred to the Instability Index (ISI) is used to investigate the level of stability/sensitivity influenced by the change of dynamics:

$$\text{ISI} = \frac{\text{std}(\chi)(\text{meter})}{l(\text{meter})} \times 100\% \qquad (33)$$

where the variable $\chi = \frac{1}{50} \sum_{i=1}^{50} \text{RMSE}_i, H$, and $\text{RMSE}_{i,}H$ represents the position root mean squared error (RMSE) for the i-th run in the H dynamic region, i.e., $H \in \{HL, HM, HH\}$, and

$$\text{std}(\chi) = \sqrt{E[(\chi - \overline{\chi})^2]} = \sqrt{\frac{1}{3} \sum_{i=1}^{3} (\chi_i - \overline{\chi})^2}$$

$$\overline{\chi} = E[\chi] = \frac{1}{3} \sum_{i=1}^{3} \chi_i$$

The ISI is simply a measure of accuracy variation among each of the three dynamic levels (HL, HM, and HH). A filter with a larger ISI value indicates that the filter is less stable/more sensitive to the change of dynamics.

Some remarks are given as follows.
(1) In the time intervals, 0-200, 401-600, 901-1200, and 1276-1600s ("L" time intervals), the vehicle is not maneuvering and is conducting constant-velocity straight-line motion. For this case, all the AUKF, IMM-UKF, and IMM-AUKF provide equivalently good results. The navigation accuracies for the three approaches lead to very similar results.
(2) In the time intervals, 201-400s (HM), 601-900s (HL), and 1200-1275s (HH), the vehicle is maneuvering. From Fig. 10 and Table 1 (a), it can be seen that the position errors for the three approaches has the relations:
- In HL interval:
$$\text{IMM - AUKF} < \text{IMM - UKF} < \text{AUKF} ;$$
- In HM and HH intervals:
$$\text{IMM - AUKF} < \text{AUKF} << \text{IMM - UKF} .$$
The IMM-UKF outperforms the AUKF in low dynamic region, while the AUKF outperforms the IMM-UKF in high dynamic region. Among the three approaches, the proposed IMM-AUKF approach has the best positioning accuracy.
(3) As shown in Fig. 11 and Table 1(b), the

standard deviations of positioning errors for IMM-UKF are large in E-HM (2.3904m) and N-HM (0.9829m), indicating that IMM-UKF occasionally performs well while sometimes gives abnormally large errors in the medium dynamic motion (HL).
(4) The ISI is an indicator of the sensitivity with respect to the change of dynamic. From Table 2, the values of the ISI measure has the relation:
$$\text{AUKF} \approx \text{IMM - AUKF} << \text{IMM - UKF} .$$
Since the AUKF has the smallest ISI value, it therefore has the best stability. On the contrary, IMM-UKF has the largest ISI value, thus is relatively sensitive to the dynamics. Overall, the IMM-AUKF gains the merits from both the IMM-UKF and AUKF, and is able to achieving promising navigation accuracy improvement and stability enhancement.
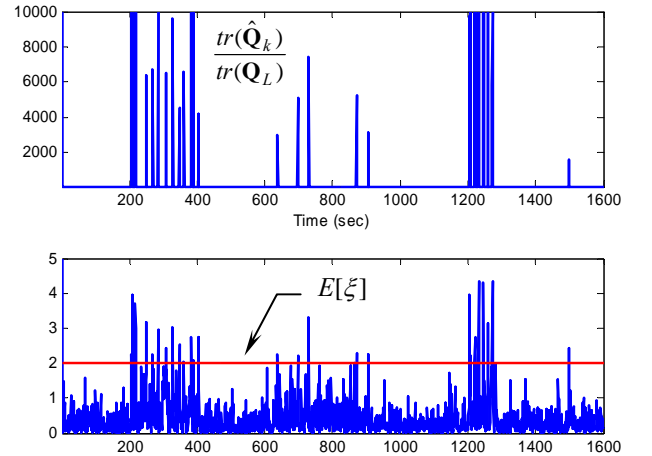
Fig. 8 The trajectories of ATS outputs (top) and the corresponding DOD parameter ξ (bottom).
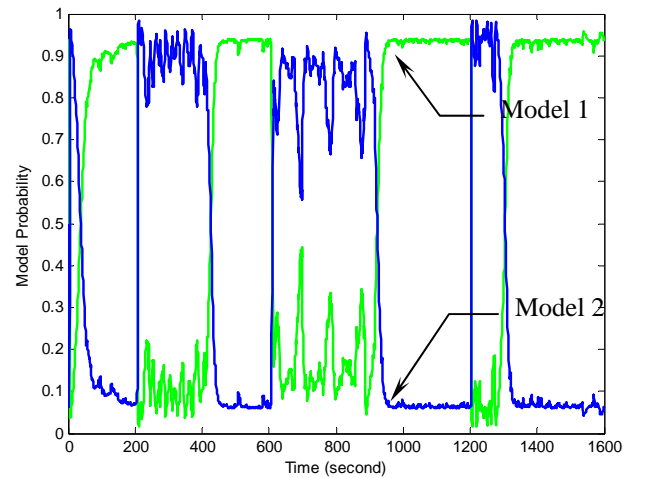
Fig. 9. Model probabilities for the IMM-AUKF.
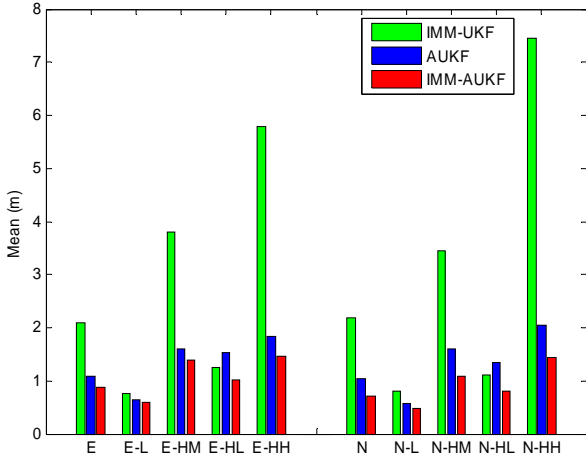
Fig. 10. Mean values of east and north position errors by IMM-UKF, AUKF, and IMM-AUKF.
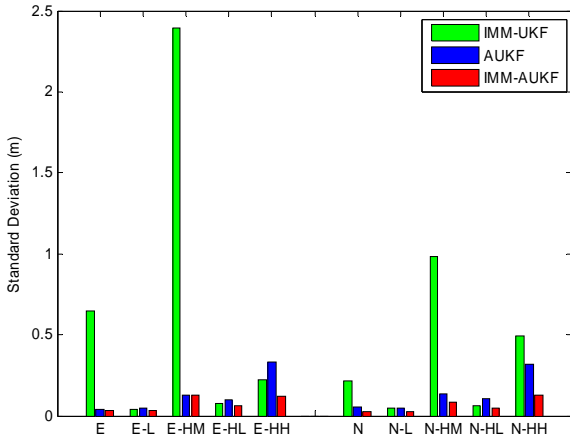
Fig. 11. Standard deviations of east and north position errors by IMM-UKF, AUKF, and IMM-AUKF.

Table 1. Mean and standard deviation of position errors for three approaches based on 50 Monte Carlo runs (in meters).

Segments		East	E-L	E-HM	E-HL	E-HH
IMM-UKF	Mean	2.0837	0.7680	3.7950	1.2576	5.7872
	Std	0.6449	0.0422	2.3904	0.0733	0.2246
AUKF	Mean	1.0920	0.6470	1.6106	1.5206	1.8343
	Std	0.0386	0.0485	0.1284	0.0989	0.3309
IMM-AUKF	Mean	0.8694	0.5892	1.3876	1.0060	1.4616
	Std	0.0332	0.0294	0.1280	0.0634	0.1211

Segments		North	N-L	N-HM	N-HL	N-HH
IMM-UKF	Mean	2.1974	0.8144	3.4463	1.1126	7.4501
	Std	0.2174	0.0462	0.9829	0.0644	0.4903
AUKF	Mean	1.0341	0.5780	1.5965	1.3353	2.0364
	Std	0.0518	0.0490	0.1361	0.1089	0.3207
IMM-AUKF	Mean	0.7137	0.4727	1.0876	0.8032	1.4271
	Std	0.0245	0.0244	0.0871	0.0512	0.1282

Table 2. Comparison of Instability Index (ISI) for three approaches.

ISI	E-(HL∪HM∪HH)	N-(HL∪HM∪HH)	Overall
IMM-UKF	185.37%	261.71%	223.54%
AUKF	13.19%	28.93%	21.06%
IMM-AUKF	19.96%	25.50%	22.73%

5 Conclusions

This paper has presented an IMM-AUKF algorithm for navigation sensor fusion. The AKF approach is featured on filter parametric adaptation, and the IMM approach is featured on structural adaptation (model switching). To solve the possible degradation problem caused by noise uncertainty and modeling error, the synthesis of two types of adaptive approaches, AKF algorithm and IMM algorithm, are proposed, leading to a new fusion method. Two models, a non-adaptive UKF and an AUKF, have been used in the IMM architecture. To adjust the bandwidth of the IMM filter, the DOD parameter ξ (defined as the normalized innovation squared value at present epoch) is used in the ATS loop for determining the upper bound of process noise covariance matrix to account for the modeling error or statistic uncertainties and accordingly enhance the estimation accuracy and tracking capability. Furthermore, a measure called the ISI has been introduced to evaluate the stability or sensitivity subject to the change of vehicle dynamics. The proposed IMM-AUKF algorithm shows robust performance in both navigational accuracy and system stability as compared to the AUKF and IMM-UKF approaches.

References

[1] Brown R and Hwang P, *Introduction to Random Signals and Applied Kalman Filtering*. John Wiley & Sons, New York, 1997.

[2] Gelb A, *Applied Optimal Estimation*. M. I. T. Press, MA, 1974.

[3] Mohamed A and Schwarz K, Adaptive Kalman filtering for INS/GPS, *Journal of Geodesy*, 73, 193-203, 1999.

[4] Hide C, Moore T, and Smith M, Adaptive Kalman filtering for low cost INS/GPS, *The Journal of Navigation*, 56(1), 143-152, 2003.

[5] Li X and Bar-Shalom Y, *Estimation with Applications*

to Tracking and Navigation. John Wiley & Sons, New York, 1993.

[6] Li X and Bar-Shalom Y, Performance prediction of the interacting multiple model algorithm, *IEEE Transactions on Aerospace and Electronic Systems*, 29(3), 755-771, 1993.

[7] Kim Y, and Hong K, An IMM algorithm for tracking maneuvering vehicles in an adaptive cruise control environment, *International Journal of Control, Automation, and Systems*, 2(3), 310-318, 2004.

[8] Lee B, Park J, Lee H, and Joo Y, Fuzzy-logic-based IMM algorithm for tracking a manoeuvring target, *IEE Proceedings-Radar Sonar Navig.*, 152(1), 16-22, 2005.

[9] Li X, and Bar-Shalom Y, Design of an interacting multiple model algorithm for air traffic control tracking, *IEEE Transactions on Control System Technology*, 1(3), 186-194, 1993.

[10] Chen G, and Harigae M, Using IMM adaptive estimator in GPS positioning, *Proceedings of the 40th SICE Annual Conference*, SICE 2001, International Session Papers, 25-27, 2001.

[11] Lin X, Kirubarajan T, Bar-Shalom Y, and Li X, Enhanced accuracy GPS navigation using the interacting multiple model estimator, *Proceedings of IEEE Aerospace Conference*, 4-1911-4-1923, 2001.

[12] Julier S, Uhlmann J, Durrant-whyte H, A new method for the nonlinear transformation of means and covariances in filters and estimators, *IEEE Transactions on Automatic Control*, 5(3), 477-482, 2000.

[13] Julier S, The scaled unscented transformation, *Proceedings of the American Control Conference*, Anchorage, USA, 4555-4559, 2002.

[14] Julier S. J. and Uhlmann J. K., Reduced sigma point filters for the propagation of means and covariances through nonlinear transformations, *Proceeding of the American Control Conference*, 887-892, 2002.

[15] Jwo D, and Lai S, Navigation integration using the fuzzy strong tracking unscented Kalman filter, *The Journal of Navigation,* 62(2), 303-322, 2009.

[16] Farrell J and Barth M, *The Global Positioning System and Inertial Navigation*, McCraw-Hill professional, 1999.

[17] Julier S, Uhlmann J, and Durrant-whyte HF, A new approach for filtering nonlinear system, *Proceeding of the American Control Conference*, 1628-1632, 1995.

[18] Wan E and van der Merwe R, The unscented Kalman filter for nonlinear estimation, in: *Proceedings of Adaptive Systems for Signal Processing, Communication and Control (AS-SPCC) Symposium*, Alberta, Canada, 153-156, 2000.

Copyright Statement